Published in final edited form as:
J Immunol. 2014 September 15; 193(6): 3113–3125. doi:10.4049/jimmunol.1400820.

Live SIV vaccine correlate of protection: local antibody production and concentration on the path of virus entry

Qingsheng Li[*,1,2], **Ming Zeng**[*,1,4], **Lijie Duan**[*,1], **James E. Voss**[†,†††,1], **Anthony J. Smith**[*,3], **Stefan Pambuccian**[‡], **Liang Shang**[*], **Stephen Wietgrefe**[*], **Peter J. Southern**[*], **Cavan S. Reilly**[§], **Pamela J. Skinner**[¶], **Mary L. Zupancic**[*], **John V. Carlis**[¤], **Michael Piatak Jr.**[#], **Diane Waterman**[**], **R. Keith Reeves**[††,‡‡], **Katherine Masek-Hammerman**[††,‡‡], **Cynthia A. Derdeyn**[§§], **Michael D. Alpert**[††,¶¶], **David T. Evans**[††,¶¶,5], **Heinz Kohler**[¤¤], **Sybille Muller**[##], **James Robinson**[***], **Jeffrey D. Lifson**[#], **Dennis R. Burton**[†,†††], **R. Paul Johnson**[††,†††], and **Ashley T. Haase**[*]

[*]Department of Microbiology, Medical School, University of Minnesota, Minneapolis, MN 55455

[†]Department of Immunology and Microbial Science, IAVI Neutralizing Antibody Center, and Center for HIV/AIDS Vaccine Immunology and Immunogen Design, The Scripps Research Institute, La Jolla, CA 92037

[‡]Department of Laboratory Medicine and Pathology, Medical School, University of Minnesota, Minneapolis, MN 55455

[§]Division of Biostatistics, School of Public Health, University of Minnesota, Minneapolis, MN 55455

[¶]Department of Veterinary and Biomedical Sciences, College of Veterinary Medicine, University of Minnesota, St. Paul, MN 55108

[¤]Department of Computer Science and Engineering, College of Science and Engineering, University of Minnesota, Minneapolis, MN 55455

[#]AIDS and Cancer Virus Program, Science Applications International Corporation–Frederick, Inc., National Cancer Institute, Frederick, MD 21702

[**]ZeptoMetrix Corporation, Buffalo, NY 14202

[††]New England Primate Research Center, Harvard Medical School, Southborough, MA, 01772

[‡‡]Infectious Disease Unit, Department of Medicine, Massachusetts General Hospital, Boston, MA 02115

Correspondence to Ashley T. Haase; phone: 612-624-4442; fax: 612-626-0623; haase001@umn.edu.
[1]Q.L., M.Z., L.D., and J.E.V. contributed equally to this work.
[2]Q. Li's present address is Nebraska Center for Virology, School of Biological Sciences, University of Nebraska, Lincoln, NE 68583.
[3]A. Smith's present address is Medical Education Review Program, DeVry Medical International, Freeport, Grand Bahama, The Bahamas.
[4]M. Zeng's present address is Center for Genetics of Host Defense, University of Texas Southwestern Medical School, Mail Code 8505, 5323 Harry Hines Boulevard, Dallas, TX 75390.
[5]D.T. Evans' present address is AIDS Vaccine Research Laboratory, Pathology and Laboratory Medicine, University of Wisconsin, 585 Science Drive, Madison, WI 53711

Conflict of interest: D. Waterman is an employee of Zeptometrix. S. Muller is an employee of ImmPheron Inc.

[§§]Department of Pathology and Laboratory Medicine and Emory Vaccine Center, Emory University, Yerkes, Atlanta, GA 30329

[¶¶]Department of Microbiology and Immunobiology, Harvard Medical School, Boston, MA 02115

[▫▫]Department of Microbiology and Immunology and Molecular Genetics, University of Kentucky, Lexington, KY 40536

[##]ImmPheron Incorporated, 5235 Athens Boonesboro Road, Lexington, Kentucky 40509

[***]Department of Pediatrics, Center for Infectious Diseases, Tulane University, New Orleans, LA 70112

[†††]Ragon Institute of Massachusetts General Hospital, Massachusetts Institute of Technology, Charlestown, MA 02129

Abstract

We sought design principles for a vaccine to prevent HIV transmission to women by identifying correlates of protection conferred by a highly effective live attenuated SIV vaccine in the rhesus macaque animal model. We show that SIVmac239Δnef vaccination recruits plasma cells and induces ectopic lymphoid follicle formation beneath the mucosal epithelium in the rhesus macaque female reproductive tract. The plasma cells and ectopic follicles produce IgG antibodies reactive with viral envelope glycoprotein gp41 trimers, and these antibodies are concentrated on the path of virus entry by the neonatal Fc receptor (FcRn) in cervical reserve epithelium and in vaginal epithelium. This local antibody production and delivery system correlated spatially and temporally with the maturation of local protection against high dose pathogenic SIV vaginal challenge. Thus, designing vaccines to elicit production and concentration of antibodies at mucosal frontlines could aid development of an effective vaccine to protect women against HIV-1.

Introduction

While there have been substantial and continuing advances in preventing HIV-1 infection, an effective HIV-1 vaccine is still critically needed, particularly to prevent transmission to the young women who bear the brunt of infection in the pandemic's epicenter in Africa (1,2). To that end, we have been seeking design principles to guide HIV-1 vaccine development by identifying correlates of the robust protection afforded by the live attenuated SIV_{mac239}Δnef vaccine (3–7) against high dose vaginal challenge in the SIV-rhesus macaque model of HIV-1 transmission to women.

To identify correlates of protection in this animal model in vivo within the female reproductive tract (FRT) tissues, we investigated the very early stages of infection and the maturation of SIV_{mac239}Δnef-associated protection for two reasons. First, existing immune responses or responses that can be deployed rapidly in early infection would be working at favorable odds against the small-infected founder populations established at the portal of entry (1). Thus, a correlate of protection might be recognizable as local innate or adaptive immune mechanisms that could inhibit the establishment and expansion of these infected founder populations. Second, SIV_{mac239}Δnef vaccination's protective effects mature over time. Animals are not significantly protected if challenged at 5 weeks following vaccination,

whereas there is sterilizing protection or attenuated infection with challenges at 15 weeks or later after vaccination (8). Thus, protection would be expected to correlate with immune responses that increase between 5 weeks and later challenge. We show here that one striking correlate of the maturation of protection at the portal of entry between 5 and 20 weeks post vaccination is a vaccine-induced system to locally produce IgG antibodies reactive with the SIV envelope glycoprotein gp41, and to concentrate these antibodies on the path of virus entry by the neonatal Fc-receptor (FcRn) (9) operating in mucosal epithelium.

Materials and Methods

Animals, vaccination, and vaginal challenge

FRT tissue correlates of protection were analyzed in tissues collected and archived in a cross-sectional serial necropsy study of 19 $SIV_{mac239}\Delta nef$ vaccinated female rhesus macaque monkeys (*Macaca mulatta*); 8 of the 19 animals were necropsied at 5 and 20 weeks post vaccination (4 animals per group) to assess the maturation of protection in FRT tissues. The remaining 11 animals were necropsied at 4, 5, 7 and 11 days post high dose vaginal challenge at 20 weeks post-vaccination. The post-challenge archived tissues from the 11 vaccinated animals were compared with FRT tissues from 11 unvaccinated animals, collected and archived from days 4–10 following vaginal challenge (10). Protection was also evaluated in a separate longitudinal study (Reeves, K.R., ms. in preparation) in which plasma VLs were monitored following vaginal challenge at 5, 20 and 40 weeks post-vaccination in 18 animals. All of the vaccinated and unvaccinated animals in the cross-sectional studies, and animals in the longitudinal study, were vaginally inoculated atraumatically twice on the same day (separated by 4 hours) with 10^5 $TCID_{50}$ in 1 ml of the same 2004 stock of SIV_{mac251}, supplied by Dr. Christopher Miller, and described in ref. 10. Animals were vaccinated by infecting intravenously with $SIV_{mac239}\Delta nef$ supplied by Dr. Ronald Desrosiers. All of the animals were housed in accordance with the regulations of the American Association of Accreditation of Laboratory Animal Care and the standards of the Association for Assessment and Accreditation of Laboratory Animal Care International at the New England and California Primate Centers. Vaccinated animals in the cross-sectional tissue and longitudinal studies were housed under identical conditions at the New England Primate Center.

Tissue collection and processing

At the time of euthanasia, tissues were collected and fixed in 4% paraformaldehyde or SafeFix II and embedded in paraffin for later sectioning and analysis. To examine the endocervical and transition zone of endocervix and ectocervix where infected cell founder populations and local expansion have been previously observed in unvaccinated animals (10–12), the uterus, cervix and vagina were dissected en block. The relevant region of cervix was dissected away from most of the uterus and vagina, and then further divided into four quadrants. Tissue pieces from each quadrant were respectively snap-frozen, fixed as described, or were used unfixed for other assays.

In situ hybridization (ISH)

In situ hybridization to detect SIV RNA^+ cells was performed as previously described (11) on twenty sections each of cervix and vagina.

Immunohistochemistry and immunofluorescence

These methods were performed as previously described (11,13). Positive stained cells or follicles were enumerated in 20 randomly acquired, high-powered images (×200 or ×400 magnification) by manually counting in each image.

RNA extraction

Frozen cervical specimens were homogenized with a power homogenizer in TRIzol without thawing. Total RNA was isolated, according to the manufacturer's protocol, and further purified with an RNeasy mini kit.

Real-time RT-PCR to determine SIV_{mac239}Δnef and WT SIV_{mac251} viral loads in tissues and plasma

RT-PCR assays were performed as described with specific primers to determine the levels of SIV_{mac239}Δnef and SIV_{mac251}, but with modifications for tissue RNA to accommodate the higher amounts and complexity of input RNA (14).

Isolation of antibodies from tissues and cervical vaginal fluids, IgG and IgA determinations and Western Blot analysis

Snap-frozen tissues were homogenized in T-PER® tissue protein extraction reagent with 1× Halt™ Protease Inhibitor, and the protein layer was collected by centrifugation. Cervical vaginal fluids were extracted from Weck-Cel sponges by eluting with 0.25% BSA and 10% Igepal (15). IgG and IgA in sera and tissue extracts were measured using ELISA commercial kits (Immunology Consultants Laboratory, Inc., Portland, OR). After incubating diluted samples in the ELISA plate, the plates were washed, incubated with anti-human IgG/IgA-HRP, again washed, developed with TMB substrate, and the absorbance was measured at 450nm. SIV-specific antibodies were detected in WB strips, normalized for total protein in the tissue extracts and sera of individual animals, and developed under conditions that maximized visualization of SIV-specific antigens with the least background. SIV-specific bands were quantified using the Bio-Rad GS-700 densitometer system, expressed as a percent of the SIV positive control band assayed concurrently, and normalized for the IgG concentrations of the tissue antibodies.

Soluble trimeric gp41

The recombinant gp41 ectodomain shown schematically in Supplementary Figure 2 was expressed in 293F cells from a phCMV plasmid that included gp160 residues 554–676 (SIV_{mac239} numbering), flanked N-terminally by an IgK signal sequence to target the protein to the ER for glycosylation, disulfide bond formation, and secretion; and C-terminally, by a strep tag for affinity purification from Freestyle 293 media using StrepTactin resin. Avidin was added to the filtered media to block biotin before loading onto the column. The column was washed with PBS, and protein eluted with 2.5mM

desthiobiotin. The eluent was loaded on a Superdex200 column to purify a 66KDa protein from higher molecular weight aggregates (approx. 1mg from 2L). This size is consistent with a trimeric quaternary structure, likely the 6-helix bundle as previously solved by X-ray crystallography and NMR (16) shown in the inset in Supplementary Figure 2b.

Reverse immunohistochemistry

For reverse immunohistochemistry staining to detect gp41-specific antibody in cells, the heat step for antigen retrieval was omitted to avoid nuclear staining artifacts. After deparaffinization and rehydration, tissue sections were blocked overnight at 4°C with SNIPER Blocking Reagent and then Avidin/Biotin Blocking Kit to minimize binding to endogeneous biotin. Sections were then incubated with Strep-tagII-labeled gp41 antigen, followed by incubation with anti Strep-tagII monoclonal antibody conjugated to HRP. Sections were then stained using DAB as substrate, counterstained with Harris Hematoxylin, and mounted in Permount. As specificity controls, the Strep-tagII monoclonal antibody alone did not stain plasma cells and reserve epithelium; or in combination with the Strep-tagII-labelled g41 did not stain these cells in FRT tissues from SIV-uninfected animals.

Neutralization assays

Protease inhibitors and the non-denaturing detergents in the tissue extracts were removed by ultrafiltration (100KD) and replaced by RPMI 1640 containing 10% normal rhesus sera. Tissue extracts and sera were serially diluted 10-fold) in RPMI 1640 containing 10% normal rhesus sera as a source of Complement, which has been reported to increase neutralization activity in sera from rhesus macaques vaccinated with $SIV_{mac239}\Delta nef$ (17). Diluted samples were co-incubated with TCLA-SIV_{mac251}, $SIV_{mac251\ 32H}$ or SIV_{mac251} vaginal challenge stock at 37°C for 1 hour before the addition of C8166–45-SEAP reporter cells (M.O.I.=0.05). The Secreted Alkaline Phosphatase (SEAP) activities were measured after 72 hours incubation (18).

In vitro culture model assessment of potential protective mechanisms

The SIV transcytosis assay was modified from ref. 19. 10^6 HEC-1A cells were seeded on 24-Transwell polycarbonate permeable membranes to establish a tight, polarized monolayer of HEC-1A cells, and monolayers were only used when the transepithelial electrical resistance was 700 Ω/cm2 or greater. Antibody-mediated blockade of transcytosis was measured in: cervical tissue extracts from vaccinated RMs; sera from vaccinated RMs or a chronically infected RM; uninfected RM sera; serum from the chronically infected RM plus Staphylococcal protein A as a competitive inhibitor of FcRn-mediated transport of IgG (20–21); and the rhesus monoclonal 4.9c antibody that reacted with oligomeric gp41 identically to the antibodies in the cervical tissues. Dilutions were added to the basolateral and apical compartments of the transwell and incubated with HEC-1A cells for 24 hours. Thereafter, $SIV_{mac251\ 32H}$ was added to the apical chamber of the transwell. Transcytosis was assessed after 6 hours and 24 hours by measuring p27 antigen in the basal chamber with a SIV p27 ELISA kit. Inhibition of SIV transcytosis was expressed as the percentage of p27 antigen recovered in the basal chamber in the presence of antibodies from different sources, compared to the amount of p27 antigen recovered in the presence of uninfected RM serum (defined as 100% transcytosis efficiency). To measure intracellular SIV p27, HEC-1A cells

were washed extensively with PBS, lysed and SIV p27 in the intracellular extracts was measured with the SIV p27 ELISA kit. For the analysis of intracellular antibody location, HEC-1 cells on the transmembrane were fixed briefly with SafeFix, permeabilized with 1% TritonX-100 and immunofluorescently stained for IgG and TOTO-3. The transmembranes with the HEC-1 cells were harvested and mounted on microscope slides using Aqua Poly/Mount. Immunofluorescent micrographs were taken using an Olympus FV1000 Fluoview confocal microscope; images were acquired and mean fluorescence intensity was analyzed using Olympus Fluoview software (version 1.7a)

Statistical methods

To test for differences between groups, pairwise 2 sample, equal variance t-tests were conducted after logarithmically transforming the data (since errors for intensity measurements are typically multiplicative) and adding the value 1 to all observations (since some measurements are zero). Differences were deemed significant if the p-value for the test is less than 0.05. All computations were done using the statistical software R version 2.10.1. Figures 6 and 8 were created in GraphPad Prism. For Figure 8g, co-localization of pixels is measured with Pearson correlation coefficients, as computed by software for the confocal microscope.

Results

Vaccination effects in the early stages of infection

$SIV_{mac239}\Delta nef$ vaccination was associated with inhibition of the establishment and local expansion of small-founder populations of SIV RNA^+ cells in the transition zone (TZ) and adjoining endocervix (10–12). In naïve-unvaccinated controls, SIV RNA^+ cells have previously been shown to be detectable as early as days 3 and 4 following high dose vaginal exposure to WT SIV_{mac251}. These founder populations then greatly expand between days 7 and 10–14 days at the peak of local replication, (Fig. 1a,c) (11,12). In striking contrast, SIV RNA^+ cells were only rarely detected in the vaccinated animals at days 4 and 5 post vaginal exposure to high doses of WT SIV_{mac251} at 20 weeks post vaccination, and there was no evidence of local expansion (Fig. 1b,d). We quantified these differences from exponential expansion to peak replication by PCR-determinations of viral tissue loads (VLs) and found that VLs in cervix and vagina were reduced from an average of 5.8×10^5 copies/μg tissue RNA in four unvaccinated animals (10) to undetectable in cervical tissues of 6/6 vaccinated animals; and undetectable in vaginal tissues of 3/6 vaccinated animals and an average of 50 copies/μg in 3/6 animals (Fig. 1e,f).

IgG antibodies to oligomeric gp41 correlate with maturation of protection

We hypothesized that SIV-specific antibodies at the portal of entry prior to challenge would be at the “right place and time” to account for the rapid inhibition of establishment and expansion of infected founder populations just described, and therefore looked for pre-challenge antibodies that increased from 5 to 20 weeks as a correlate of the maturation of the protective effects of vaccination. Consistent with this hypothesis, we detected predominantly IgG antibodies reactive with SIV oligomeric gp41 in Western blots (WB) prior to WT SIV_{mac251} vaginal challenge that significantly ($p<0.01$) increased 5-fold between 5 and 20

weeks in cervical, vaginal tissues and CVF (Fig. 2 a,c,d). The gp160 and gp80 bands with which the antibodies reacted most strongly in cervical vaginal tissues and fluids and in serum (Fig. 2e) were shown two decades ago to be oligomeric complexes of gp41 (22–24). This conclusion was further supported by reactivity with rhesus monoclonal antibodies to gp41 but not gp120 (25) (Fig. 2b), and indeed identical reactivity with oligomeric gp41 in WBs of monoclonal antibody 4.9C and antibodies in the FRT (indicated by the red box in Fig. 2b). Cervical IgG antibodies reactive with gp41IgA antibodies reacting mainly with oligomeric gp41also increased between 5 and 20 weeks in the cervical vaginal tissue extracts, CVF and serum (not shown). However, because IgA concentrations were 150 to 200-fold lower than IgG (Supplemental Table 1), we subsequently focused on the role IgG antibodies might be playing in the temporal maturation of protection.

Cervical IgG antibody production and delivery

We initially stained sections to see if IgG antibodies might be detectable at the tissue sites where the inhibition of viral replication had been observed. We discovered by this simple approach that the numbers of IgG^+ cells in the cervix increased in the vaccinated animals compared to unvaccinated SIV-negative controls and between 5 and 20 weeks in the vaccinated animals (Fig. 3 a,b; Supplemental Fig. 1a). The IgG^+ cells in the submucosa were identified as plasma cells by their morphology, and by staining for a plasma cell marker, CD138 (26) (not shown), whereas the IgG^+ cells just beneath the columnar epithelium lining the cervix were identified as epithelial reserve cells (27) by: 1) their epithelial morphology; 2) location in the TZ and adjoining endocervix (Fig. 3b), and 3) by co-localization of IgG staining with the reserve cell marker (28), cytokeratin 5 (CK5) (Fig. 3 c,d).

The images of the location of IgG in the reserve epithelium struck us as somewhat similar to images of the FcRn in murine and human uterine and vaginal epithelium (29). We therefore hypothesized that the rhesus macaque cervical reserve epithelium might express $FcRn^+$, and tested this hypothesis by staining cervical sections with antibody to FcRn. We indeed found that IgG and the FcRn co-localized in CK5+cervical reserve epithelium (Fig. 3e–h). IgG^+-staining plasma cells increased about 2.5-fold and cervical reserve epithelium more than 10-fold between 5 and 20 weeks (Fig. 3i).

Local gp41t antibody production and delivery

We had thus visualized a potentially generic system for local production and concentration of IgG antibodies in the TZ of the cervix. To show that such a system concentrated gp41-specific IgG antibodies at the portal of entry, we used reverse immunohistochemistry (RIHC) (30) to stain cells containing gp41 antibodies. For RIHC-staining, we generated a soluble trimeric gp41 (sgp41t) ectodomain recombinant protein, which was designed to mimic *in vivo* antigens, such as trimeric gp41 6-helical bundles (“stumps”) left in the viral membrane following gp120 shedding (31). The sgp41t protein retained cluster I and II immunodominant epitopes (32,33), but lacked the hydrophobic transmembrane domain, the membrane proximal external region (MPER), and fusion peptide regions of gp41 (Supplementary Fig. 2). With this reagent, we found that gp41t-antibodies were readily detectable in plasma cells and $FcRn^+$ cervical reserve cells (Fig. 4 a–d) in 4 of 4 animals at 20 weeks, but only faint staining compared to naïve controls (Fig. 4 e, f) in 4 animals at 5

weeks (Fig. 5). The increased staining of reserve epithelium at 20 weeks compared to 5 weeks is consistent with: 1) the increased gp41t$^+$ plasma cells in the submucosa; 2) increased antibodies to gp41t present in the tissues and CVF (Fig. 2); and 3) maturation of protection.

Vaginal IgG antibody production and delivery

We next showed that there is a system in the vagina to locally produce and concentrate IgG antibodies comparable to the endocervix. In the vagina, IgG$^+$ cells beneath the epithelium increased in the vaccinated animals compared to unvaccinated SIV-negative controls (Supplemental Fig. 1b) and between 5 and 20 weeks in the vaccinated animals (Fig. 6 a,b). The IgG$^+$ cells were identified as plasma cells by their morphology and by staining with the plasma cell marker, CD138 (Supplemental Fig. 3). In addition, there were also ectopic tertiary lymphoid follicles in the vagina containing IgG$^+$ and gp41t- antibody$^+$ plasma cells (Fig. 6 c,d) that increased in number by 9-fold between 5 and 20 weeks (Fig. 6e). Because murine vaginal epithelial cells are a known source of chemokines that recruit CTLs to the FRT (34), we asked whether epithelium might be a source of chemokines to recruit plasma cells in rhesus macaques. We indeed found that expression of CXCL10 at 20 weeks in vaginal multilayered squamous epithelium (Fig. 6f) was associated with recruitment of CXCR3$^+$ plasma cells to vaginal submucosa and into follicles (Fig. 6 g,h). Similarly, CXCL10 expression increased in endocervical epithelium between 5 and 20 weeks as a mechanism to recruit plasma cells to that site (Fig. 6i).

The neonatal Fc receptor was also constitutively expressed at approximately comparable levels at 5 and 20 weeks post vaccination in the vagina and ectocervix. FcRn-expression was mainly in the basal layers of the multilayered squamous epithelium (Fig. 6 j,k), in close proximity to the plasma cells and follicles producing IgG antibodies. The image shown of IgG concentrated in basal epithelium above the IgG$^+$ cells in the submucosa at 20 weeks post vaccination (Fig. 6l) is consistent with the proposed system in which spatial proximity between cells producing IgG antibodies to FcRn-expressing epithelium could concentrate antibodies to intercept virus that has traversed the mucosal barrier to that depth.

Potential protective mechanisms for gp41t antibodies in the FRT

The gp41t antibodies are thus located at the right time and right place to intercept virus at entry and immediately contain infection by a number of mechanisms. These include classical extracellular neutralization (35) and intracellular neutralization (36) in which virus captured by IgG bound to FcRn is diverted from the early endosome pathway and degraded in lysosomes; and virus binding and capture (37). We investigated neutralization in vitro in assays using unheated sera as a source of complement (17). The 20-week sera neutralized Tissue Culture Lab-Adapted (TCLA)-SIV$_{mac251}$ at higher titer than at 5 weeks (Fig. 7a). However, activity against the somewhat more neutralization-resistant SIV$_{mac251\text{-}32H}$ strain, or the challenge stock of SIV$_{mac251}$ was weaker and did not differ significantly between 5 and 20 weeks. We interpret reductions in viral infectivity of only 50 percent over a broad range of dilutions at 20 weeks as plateau effects of a neutralization resistant fraction of virus (Fig. 7 b,c).

Virus-capture and intracellular neutralization was assayed in $FcRn^+$ HEC 1-A cells in a transwell system (19) to mimic in vitro these activities in cervical reserve and vaginal epithelium (Fig. 8a). We tested sera from a chronically infected animal as a positive control in this assay, as well as the rhesus monoclonal antibody, 4.9C, because of the similar reactivity of that antibody and anti-oligomeric gp41 antibodies in WBs (Fig. 2b). IgG and FcRn co-localized in an early endosomal pathway in this assay system (Fig. 8b), as did IgG from the positive control sera and SIV (Fig. 8c), and a significantly greater fraction of the SIV captured by positive control sera compared to sera from uninfected animals was diverted to $LAMP1^+$ lysosomes for degradation (Fig. 8d,g), as described for intracellular neutralization (36). Positive control sera, 20-week sera and cervical tissue extracts, and monoclonal antibody 4.9C all significantly decreased transcytosis in this system, whereas sera from uninfected animals and 5-week sera and tissue extracts did not (Fig. 8e,f). We showed that the FcRn-translocation pathway was involved in capture and transcytosis by reversing these activities with Staphylococcal protein A (SA) binding of IgG, which acts as a competitive inhibitor of FcRn-mediated transport (Fig. 8e,f) (20,21).

Discussion

As one of the interfaces with the external environment, the mucosa of the female reproductive tract has evolved multiple mechanisms to protect against pathogens. Here we describe a spatial and temporal correlate of the maturation of protection against high dose vaginal challenge conferred by vaccination with an effective live attenuated vaccine. We found that vaccination with SIVΔnef induced an organized system of local antibody production and concentration that correlated with reduction in VLs in the FRT tissues to undetectable or very low levels in vaccinated compared to unvaccinated animals. In the cervix, local production by plasma cells underlying $FcRn^+$ cervical reserve epithelium comprise a system to deliver and concentrate gp41t IgG antibodies at a critical site and time where establishment and expansion of infected founder populations precedes production of sufficient virus and infected cells to disseminate and rapidly establish a robust systemic infection (1,10–12). In the vagina, antibody production and delivery by plasma cells and ectopic follicles underlying $FcRn^+$ basal epithelium would similarly concentrate gp41t antibodies as a second line of defenses to prevent viruses traversing the multilayered squamous epithelial barrier from infecting target cells in the underlying submucosa.

There are four important components of this antibody correlate of local protection induced by SIVΔnef vaccination (Fig. 9): 1) recruitment of plasma cells and formation of ectopic follicles; 2) local production of gp41t antibodies; 3) FcRn-mediated mechanisms in cervical reserve and basal vaginal epithelium to concentrate SIV-specific IgG antibody to intercept virus on entry and inhibit the necessary interactions with target cells to establish infection at the portal of entry; and 4) an active role for the mucosal epithelium lining the cervix and vagina in recruiting plasma cells and increasing ectopic follicles as well as concentrating antibodies by FcRn-mediated mechanisms.

One critical feature of this system is locating a production source in close proximity to the delivery system. This feature in principle overcomes diffusion constraints for antibodies coming from the circulation to achieve the high local concentration of antibodies to intercept

virus at entry by mass action mechanisms we next describe. We also note here that direct visualization of gp41t-staining of reserve epithelium is consistent with the idea that we can see IgG antibodies in the cells because the high local concentrations exceed the normal FcRn-flux rate for IgG of multiple specificities.

Antibody production and concentration in the FRT could likely protect through multiple cooperative, complementary and non-exclusive mechanisms. We think the most important of these mechanisms is an example of the general principle of concentration dependent protection at mucosal frontlines. This concept provides a theoretical framework to understand the increased efficacy of protection against acquisition by passive immunization with more potent new generation monoclonal antibodies against HIV (38); and the importance of the FcRn in protecting mice against HSV-2 infection (29). For SIVΔnef, we think this principle applies through the cooperative “mass action” effects of the high local concentrations of reactants-antibody and virus-in the small volume where they would first interact at the portal of entry. These concentration-dependent effects might amplify in vivo what appear from in vitro assays to be relatively weak extracellular neutralization, and might similarly amplify protective mechanisms related to virus binding and trapping to prevent access to susceptible target cells (39).

What are the similarities and differences between this system of local antibody production and concentration as a correlate of SIVΔnef’s robust protection and other potential mechanisms of protection? First, vaginal IgG antibodies with neutralizing or ADCC activity have been shown to protect against vaginal SHIV challenge (40). However, these antibodies were elicited by immunization with a gp41 trimer-peptide from which the immunodominant cluster I epitope had been deleted. In contrast, IgG antibodies to gp41t elicited by SIVΔnef are more reminiscent of the HIV-1 monoclonal antibody F240 (35), which strongly binds to the Cluster 1 epitope. Moreover, ADCC activity and NK cell and macrophage numbers as ADCC effector in cervical vaginal tissues do not correlate with the maturation of SIVΔnef protection (Alpert, M, Evans, D., *et al*., unpublished; Shang, L., *et al*., *Journal of Immunology*, in press). Second, the FcRn pathway has been utilized to enhance antigen presentation and the B and T cell responses in the mouse to HIV-Gag as well as deliver passively transferred antibodies that increased protection against HSV-2 infection (29,41,42). However, there is no evidence that these strategies reproduced the SIVΔnef system of local antibody production and concentration. Lastly, a new chemokine “pull” strategy for recruiting T cells to the genital tract has been shown to enhance local protection against HSV-2 in mice (43). By contrast, we do not find an increase in SIV-specific CD8 T cells in the FRT as a correlate of the maturation of protection with SIVΔnef vaccination (44).

The robust protection afforded by live attenuated SIV vaccines (4–7) provides motive and rationale to identify correlates of that protection to guide development of HIV-1 vaccine candidates that would circumvent the safety issues (45,46) associated with SIVΔnef vaccination. Reproducing the system described here of local antibody production and concentration at mucosal frontlines is thus a promising design principle to incorporate into the development and assessment of vaccines to prevent HIV-1 transmission to women.

Supplementary Material

Refer to Web version on PubMed Central for supplementary material.

Acknowledgments

We thank R. Desrosiers and C. Miller for virus stocks; C. Miller for tissue samples from uninfected animals and from unvaccinated and infected animals; A. Carville for expert veterinary care; E. Curran and A. Miller for assistance with tissue processing and analysis; J. Estes, E. Hunter, A. Iwasaki, D. Montefiori, J. Moore, G. Spear, C. Wira, and S. Zolla-Pazner for helpful discussions; and C. O'Neill and T. Leonard for help in preparing the manuscripts and figures. The AIDS Research and Reference Reagent Program, Division of AIDS, NIAID, NIH provided $SIV_{mac251\ 32H}$ from Drs. M. Cranage and R. Desrosiers and SIV_{mac251} antiserum from Drs. K. Reimann and D. Montefiori.

This work was supported by a grant to A. T. H. from the International AIDS Vaccine Initiative, and NIH grants AI 086922 to A. T. H., AI 071306 and RR00168 to R. P. J., AI095985 to R. P. J. and A. T. H, AI 055332 and1UM1AI100663 to D. R. B., a CHAVI/HVTN Early Stage Investigator award, and grant number U19 AI 067854, to R. K. R., a Ragon Fellowship to J. V., and with federal funds from the National Cancer Institute, National Institutes of Health, under contract HHSN261200800001E and the NIH/NIAID Reagent Resource Support Program for AIDS Vaccine Development, Quality Biological, Inc., Gaithersburg, MD (DAIDS Contract Number HHSN272201100023C).

Abbreviations used

CK5	cytokeratin 5
CVF	cervical vaginal tissues and fluid
FcRn	neonatal Fc receptor
FRT	female reproductive tract
ISH	in situ hybridization
MPER	membrane proximal external region
RIHC	reverse immunohistochemistry
SEAP	secreted alkaline phosphatase
sgp41t	soluble trimeric gp41
SIV	simian immunodeficiency virus
TCLA	Tissue Culture Lab-Adapted
TZ	transition zone
WB	Western blot

References

1. Haase AT. Targeting early infection to prevent HIV-1 mucosal transmission. Nature. 2010; 464:217–223. [PubMed: 20220840]
2. Quinn TC, Overbaugh J. HIV/AIDS in women: an expanding epidemic. Science. 2005; 308:1582–1583. [PubMed: 15947174]
3. Daniel MD, Kirchhoff F, Czajak SC, Sehgal PK, Desrosiers RC. Protective effects of a live attenuated SIV vaccine with a deletion in the *nef* gene. Science. 1992; 258:1938–1941. [PubMed: 1470917]

4. Johnson RP. Live attenuated AIDS vaccines: hazards and hopes. Nat. Med. 1999; 5:154–155. [PubMed: 9930861]

5. Koff WC, Johnson RP, Watkins DW, Burton DR, Lifson JD, Hasenkrug KJ, McDermott AB, Schultz A, Zamb TJ, Boyle R, Desrosiers RC. HIV vaccine design: insights from live atenuated SIV vaccines. Nat. Immunol. 2006; 7:19–23. [PubMed: 16357854]

6. Reynolds MR, Weiler AM, Weisgrau KL, Piaskowski SM, Furlott JR, Weinfurter JT, Kaizu M, Soma T, Leon EJ, MacNair C, Leaman DP, Zwick MB, Gostick E, Musani SK, Price DA, Friedrich TC, Rakasz EG, Wilson NA, McDermott AB, Boyle R, Allison DB, Burton DR, Koff WC, Watkins DI. Macaques vaccinated with live-attenuated SIV control replication of heterologous virus. J. Exp. Med. 2008; 205:2537–2550. [PubMed: 18838548]

7. Reynolds MR, Weiler AM, Piaskowski SM, Kolar HL, Hessell AJ, Weiker M, Weisgrau KL, Leon EJ, Rogers WE, Makowsky R, McDermott AB, Boyle R, Wilson NA, Allison DB, Burton DR, Koff WC, Watkins DI. Macaques vaccinated with simian immunodeficiency virus SIVmac239Δnef delay acquisition and control replication after repeated low-dose heterologous SIV challenge. J. Virol. 2010; 84:9190–9199. [PubMed: 20592091]

8. Connor RI, Montefiori DC, Binley JM, Moore JP, Bonhoeffer S, Gettie A, Fenamore EA, Sheridan KE, Ho DD, Dailey PJ, Marx PA. Temporal analyses of virus replication, immune responses, and efficacy in rhesus macaques immunized with a live, attenuated simian immunodeficiency virus vaccine. J. Virol. 1998; 72:7501–7509. [PubMed: 9696847]

9. Roopenian DC, Akilesh S. FcRn: the neonatal Fc receptor comes of age. Nat. Rev. Imm. 2007; 7:716–725.

10. Miller CJ, Li Q, Abel K, Kim E-Y, Ma Z-M, Wietgrefe S, LaFranco-Scheuch L, Compton L, Duan L, Shore MD, Zupancic M, Busch M, Carlis J, Wolinsky S, Haase AT. Propagation and dissemination of infection after vaginal transmission of simian immunodeficiency virus. J. Virol. 2005; 79:9217–9227. [PubMed: 15994816]

11. Li Q, Estes JD, Schlievert PM, Duan L, Brosnahan AJ, Southern PJ, Reilly CS, Peterson ML, Schultz-Darken N, Brunner KG, Nephew KR, Pambuccian S, Lifson JD, Carlis JV, Haase AT. Glycerol monolaurate prevents mucosal SIV transmission. Nature. 2009; 458:1034–1038. [PubMed: 19262509]

12. Zhang ZQ, Schuler T, Zupancic M, Wietgrefe S, Reimann KA, Reinhart TA, Rogan M, Cavert W, Miller CJ, Veazey RS, Notermans D, Little S, Danner SA, Richman DD, Havlir D, Wong J, Jordan HL, Schacker TW, Racz P, Tenner-Racz K, Letvin NL, Wolinsky S, Haase AT. Sexual transmission and propagation of simian and human immunodeficiency viruses in two distinguishable populations of $CD4^+$ T cells. Science. 1999; 286:1353–1357. [PubMed: 10558989]

13. Zeng M, Smith AJ, Wietgrefe SW, Southern PJ, Schacker TW, Reilly CS, Estes JD, Burton GF, Silvestri G, Lifson JD, Carlis JV, Haase AT. Cumulative mechanisms of lymphoid tissue fibrosis and T cell depletion in HIV-1 and SIV infections. J. Clin. Invest. 2011; 121:998–1008. [PubMed: 21393864]

14. Salisch NC, Kaufmann DE, Awad AS, Reeves RK, Tighe DP, Li Y, Piatak M Jr, Lifson JD, Evans DT, Pereyra F, Freeman GJ, Johnson RP. Inhibitory TCR coreceptor PD-1 is a sensitive indicator of low-level replication of SIV and HIV-1. J. Immunol. 2010; 184:476–487. [PubMed: 19949078]

15. Kozlowski PA, Lynch RM, Patterson RR, Cu-Uvin S, Flanigan TP, Neutra MR. Modified wick method using Weck-Cel sponges for collection of human rectal secretions and analysis of mucosal HIV antibody. J. Acquir. Immune Defic. Syndr. 2000; 24:297–309. [PubMed: 11015145]

16. Caffrey M, Cai M, Kaufman J, Stahl SJ, Wingfield PT, Covell DG, Gronenborn AM, Clore GM. Three-dimensional solution structure of the 44 kDa ectodomain of SIV gp41. EMBO J. 1998; 17:4572–4584. [PubMed: 9707417]

17. Freissmuth D, Hiltgartner A, Stahl-Hennig C, Fuchs D, Tenner-Racz K, Racz P, Uberta K, Strasak A, Dietrich MP, Stolber H, Falkensammer B. Analysis of humoral immune responses in rhesus macaques vccinated with attenuated SIVmac239Δnef and challenged with pathogenic SIVmac251. J. Med. Primatol. 2010; 39:97–111. [PubMed: 20015159]

18. Means RE, Greenough T, Desrosiers RC. Neutralization sensitivity of cell culture-passaged simian immunodeficiency virus. J. Virol. 1997; 71:7895–7902. [PubMed: 9311879]

19. Shen R, Drelichman ER, Bimczok D, Ochsenbauer C, Kappes JC, Cannon JA, Tudor D, Bomsel M, Smythies LE, Smith PD. GP41-specific antibody blocks cell-free HIV type 1 transcytosis

through human rectal mucosa and model colonic epithelium. J. Immunol. 2010; 184:3648–3655. [PubMed: 20208001]

20. Atohe F, Radulescu L, Gafencu A, Ghetie V, Simionescu M. Expression of functionally active FcRn and the differentiated bidirectional transport of IgG in human placental endothelial cells. Human Immunol. 2001; 62:93–105. [PubMed: 11182218]
21. Maidji E, McDonagh S, Genbacev O, Tabata T, Pereira L. Maternal antibodies enhance or prevent cytomegalovirus infection in the placenta by neonatal Fc receptor-mediated transcytosis. Am. J. Pathol. 2006; 168:1210–1226. [PubMed: 16565496]
22. Pinter A, Honnen WJ, Tilley SA, Bona C, Zaghouani H, Gorny MK, Zolla-Pazner S. Oligomeric structure of gp41, the transmembrane protein of human immunodeficiency virus type 1. J. Virol. 1989; 63:2674–2679. [PubMed: 2786089]
23. Zolla-Pazner S, Gorny MK, Honnen WJ, Pinter A. Reinterpretation of human immunodeficiency virus Western blot patterns. N. Engl. J. Med. 1989; 320:1280–1281. [PubMed: 2710209]
24. Parekh BS, Pau CP, Granade TC, Rayfield M, DeCock KM, Gayle H, Schoechetman G, George JR. Oligomeric nature of transmembrane glycoproteins of HIV-2: procedures for their efficient dissociation and preparation of Western blots for diagnosis. AIDS. 1991; 5:1009–1013. [PubMed: 1777159]
25. Cole KS, Alvarez M, Elliott DH, Lam H, Martin E, Chau T, Micken K, Rowles JL, Clements JE, Murphey-Corb M, Montelaro RC, Robinson JE. Characterization of neutralization epitopes of simian immunodeficiency virus (SIV) recognized by rhesus monoclonal antibodies derived from monkeys infected with an attenuated SIV strain. Virology. 2001; 290:59–73. [PubMed: 11883006]
26. Sanderson RD, Lalor P, Bernfield M. B lymphocytes express and lose syndecan expession at specific stages of differentiation. Cell Regulation. 1989; 1:27–35. [PubMed: 2519615]
27. Smedts F, Ramaekers F, Troyanovsky S, Pruszczynski M, Robben H, Lane B, Leigh I, Plantema F, Vooijs P. Basal cell keratins in cervical reserve cells and a comparison to their expression in cervical intraepithelial neoplasia. Am. J. Pathol. 1992; 140:601–612. [PubMed: 1372156]
28. Martens JE, Smedts FM, Ploeger D, Helmerhorst TJ, Ramaekers Fc, Arends JW, Hopman AH. Distribution pattern and marker profile show two subpopulations of reserve cells in the endocervical canal. Int. J. Gynecol. Pathol. 2009; 28:381–388. [PubMed: 19483623]
29. Li Z, Palaniyandi S, Zeng R, Tuo W, Roopenian DC, Zhu X. Transfer of IgG in the female genital tract by MHC class I-related neonatal Fc receptor (FcRn) confers protective immunity to vaginal infection. Proc. Natl. Acad. Sci. USA. 2011; 108:4388–4393. [PubMed: 21368166]
30. Tsuge S, Mizutani Y, Matsuoka K, Sawasaki T, Endo Y, Naruishi K, Maeda H, Takashiba S, Shiogama K, Inada K, Tsutsumi Y. Specific in situ visualization of plasma cells producing antibodies against *Porphyromonas gingivalis* in gingival radicular cyst: Application of the enzyme-labeled antigen method. J. Histochem. Cytochem. 2011; 59:673–689. [PubMed: 21525188]
31. Moore PL, Crooks ET, Porter L, Zhu P, Cayanan CS, Grise H, Corcoran P, Zwick MB, Franti M, Morris L, Roux KH, Burton DR, Binley JM. Nature of nonfunctional envelope proteins on the surface of human immunodeficiency virus type 1. J. Virol. 2006; 80:2515–2528. [PubMed: 16474158]
32. Zolla-Pazner S. Identifying epitopes of HIV-1 that induce protective antibodies. Nat. Rev. Immunol. 2004; 4:199–210. [PubMed: 15039757]
33. Xu J-Y, Gorny MK, Palker T, Karwaska S, Zolla-Pazner S. Epitope mapping of two immunodominent domains of gp41, the transmembrane protein of HIV-1. Using ten human monoclonal antibodies. J. Virol. 1991; 65:4832–4838. [PubMed: 1714520]
34. Nakanishi Y, Lu B, Gerard C, Iwasaki A. $CD8^+$ T lymphocyte mobilization to virus-infected tissue requires $CD4^+$ T cell help. Nature. 2009; 462:510–514. [PubMed: 19898495]
35. Burton DR, Hessell AJ, Keele BF, Klasse PJ, Ketas TA, Moldt B, Dunlop DC, Poignard P, Doyle LA, Cavacini L, Veazey RS, Moore JP. Limited or no protection by weakly or nonneutralizing antibodies against vaginal SHIV challenge of macaques compared with a strongly neutralizing antibody. Proc. Nat. Acad. Sci. USA. 2011; 108:11181–11186. [PubMed: 21690411]

36. Bai Y, Ye L, Tesar DB, Song H, Zhao D, Bjorkman PJ, Roopenian DC, Zhu X. Intracellular neutralization of viral infection in polarized epithelial cells by neonatal Fc receptor-mediated IgG transport. Proc. Nat. Acad. Sci. USA. 2011; 108:18406–18411. [PubMed: 22042859]
37. Burrer R, Haessig-Einius S, Aubertin A-M, Moog C. Neutralizing as well as non-neutralizing polyclonal immunoglobulin (Ig)G from infected patients capture HIV-1 via antibodies directed against the principal immunodominant domain of gp41. Virology. 2005; 333:102–113. [PubMed: 15708596]
38. Shingai M, Nishimura Y, Klein F, Mouquet H, Donau O, Plishka R, Buckler-White A, Seaman M, Piatek M Jr, Lifson J, Dimitrov D, Nussenzweig M, Martin M. Antibody-mediated immunotherapy of macaques chronicallyinfected with SHIV suppresses viraemia. Nature. 2013; 503:277–280. [PubMed: 24172896]
39. Hope T. To neutralize or not, a key HIV vaccine question. Nat. Med. 2011; 17:1195–1197. [PubMed: 21988997]
40. Bomsel M, Tudor D, Drillet AS, Alfsen A, Ganor Y, Roger MG, Mouz N, Amacker M, Chalifour A, Diomede L, Devillier G, Cong Z, Wei Q, Gao H, Qin C, Yang GB, Zurbriggen R, Lopalco L, Fleury S. Immunization with HIV-1 gp41 subunit virosomes induces mucosal antibodies protecting nonhuman primates against vaginal SHIV challenges. Immunity. 2011; 34:269–280. [PubMed: 21315623]
41. Ye L, Zeng R, Bai Y, Roopenian DC, Zu X. Efficient mucosal vaccination mediated by the neonatal Fc receptor. Nat. Biotechnol. 2011; 29:158–163. [PubMed: 21240266]
42. Lu L, Palaniyandi S, Zeng R, Bai Y, Liu X, Wang Y, Pauza CD, Roopenian DC, Zhu X. A neonatal Fc receptor-targeted mucosal vaccine strategy effectively induces HIV-1 antigen-specific immunity to genital infection. J. Virol. 2011; 85:10542–10553. [PubMed: 21849464]
43. Shin H, Iwasaki A. A vaccine strategy that protects against genital herpes by establishing local memory T cells. Nature. 2012; 491:463–467. [PubMed: 23075848]
44. Sasikala-Appukuttan AK, Kim HO, Kinzel NJ, Hong JJ, Smith AJ, Wagstaff R, Reilly C, Piatak M Jr, Lifson JD, Reeves RK, Johnson RP, Haase AT, Skinner PJ. Location and dynamics of the immunodominant CD8 T cell response to SIVΔnef immunization and SIVmac251 vaginal challenge. PLoS One. 2013; 8(12):e81623. [PubMed: 24349100]
45. Baba T, Jeong YS, Penninck D, Bronson R, Greene MF, Ruprecht RM. Pathogenicity of live, attenuated SIV after mucosal infection of neonatal macaques. Science. 1995; 267:1820–1825. [PubMed: 7892606]
46. Baba TW, Liska V, Khimani AH, Ray NB, Dailey PJ, Penninck D, Bronson R, Greene MF, McClure HM, Martin LN, Ruprecht RM. Live attenuated, multiply deleted simian immunodeficiency virus causes AIDS in infant and adult macaques. Nat. Med. 1999; 5:194–203. [PubMed: 9930868]

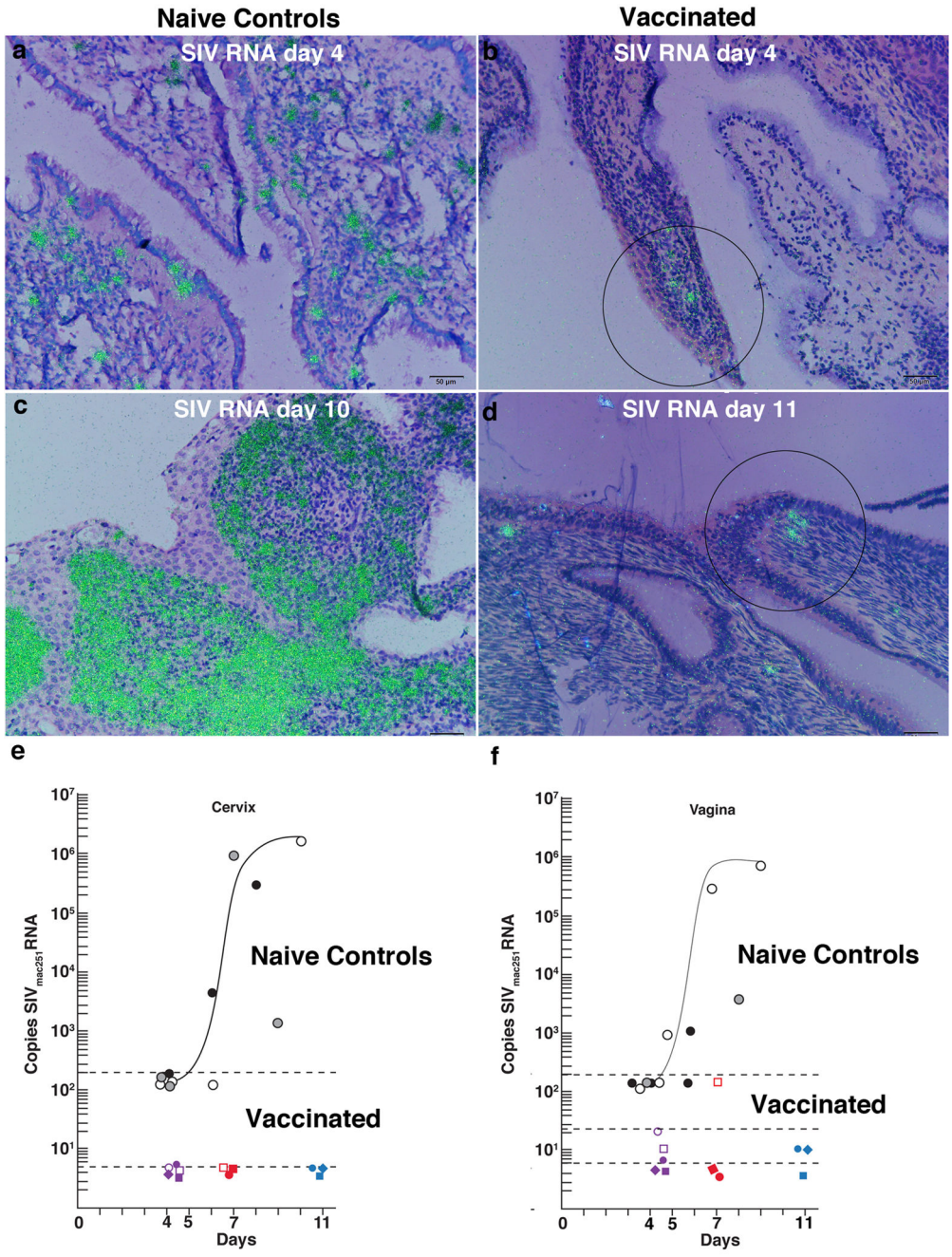

FIGURE 1.

Vaccine-associated inhibition of infection in the cervix and vagina. (**a**) Founder population of SIV RNA$^+$ cells (green) detected by ISH in the cervix of an unvaccinated animal 4 days after high dose vaginal inoculation with SIV$_{mac251}$. (**b**) Small focus of SIV RNA$^+$ cells (encircled) in a vaccinated animal at 4 days after vaginal challenge with SIV as described in (**a**). (**c**) Local expansion of SIV RNA$^+$ cells in the cervix, naïve control, at day 10, peak viral replication. (**d**) No local expansion in vaccinated animals post vaginal challenge. Three SIV RNA$^+$ cells encircled. (**e, f**) Copies of SIV$_{mac251}$/μg cervical and vaginal tissue RNA,

plotted against days post vaginal challenge through peak. Filled or unfilled black and gray circles represent individual unvaccinated animal controls (10). Copy numbers for individual vaccinated animals are indicated by colored symbols. The curved line depicts an in vivo growth curve for these tissues in unvaccinated animals. The black dotted lines indicate the limits of detection of the assays at the times they were performed.

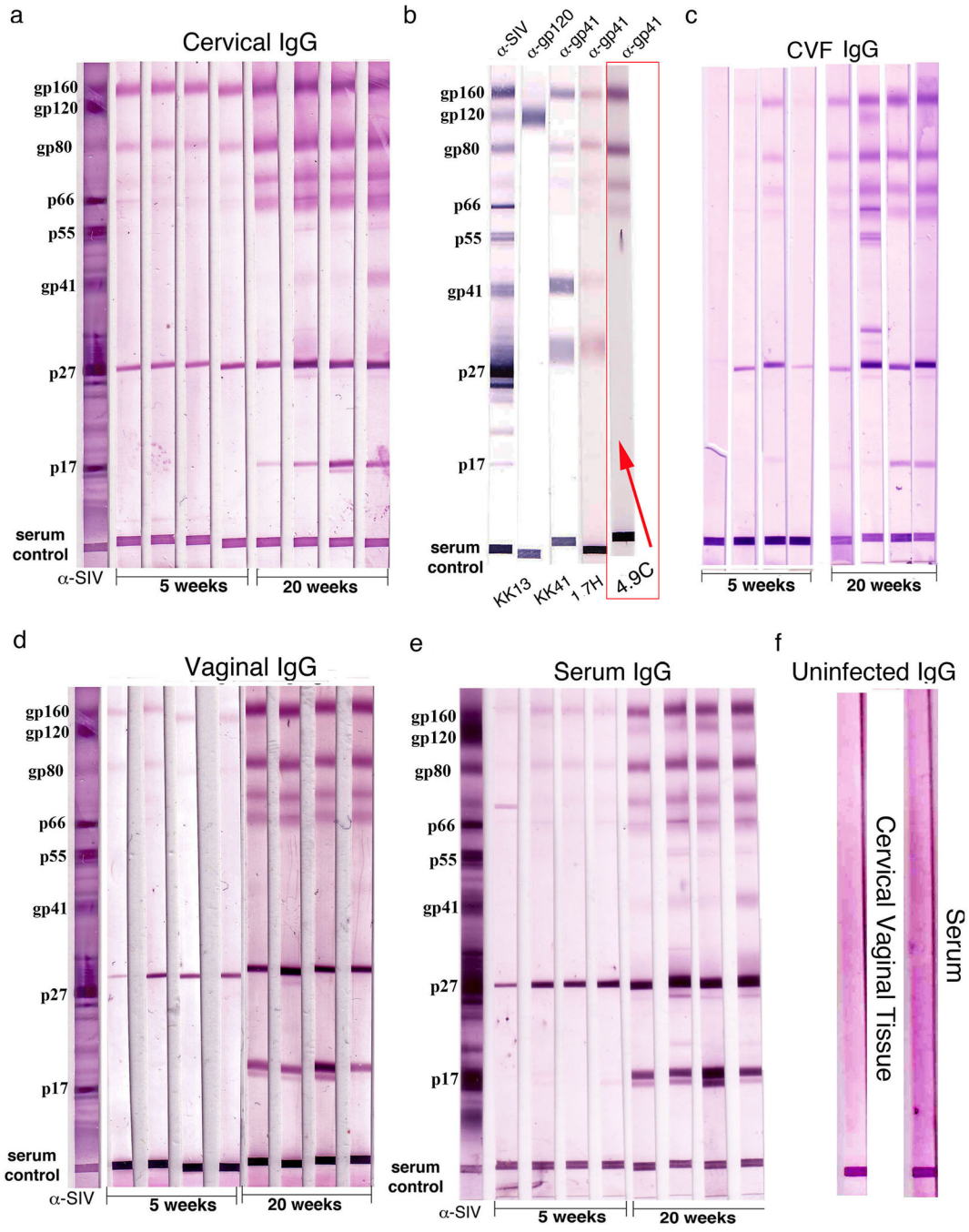

FIGURE 2.

Increased SIV-gp41 IgG antibodies correlate with the temporal maturation of protection. Each lane in the WBs represents an individual animal. (**a, c, d**) Increases between 5 and 20 weeks in IgG-antibodies in cervical vaginal tissue extracts or fluids reacting with oligomeric Env gp41antigens-gp160, gp80, and two other glycoproteins of lower molecular wt. Lanes marked α–SIV indicate positive control polyclonal antibody; serum control indicates that sample was loaded. (**b**) Rhesus monoclonal antibodies to gp41 and gp120 identify prominent Env antigen bands as oligomeric gp41. The band at ~31 kDa is thought to be a truncated

species of gp41. The WB lane with a rhesus monoclonal antibody, 4.9C, which reacts identically to cervical tissue antibodies to oligomeric gp41, is indicated by a red box and arrow. (**e**) Similar increases and SIV-reactivities in IgG in serum. (**f**) Cervical vaginal tissue and serum controls, SIV-uninfected tissues.

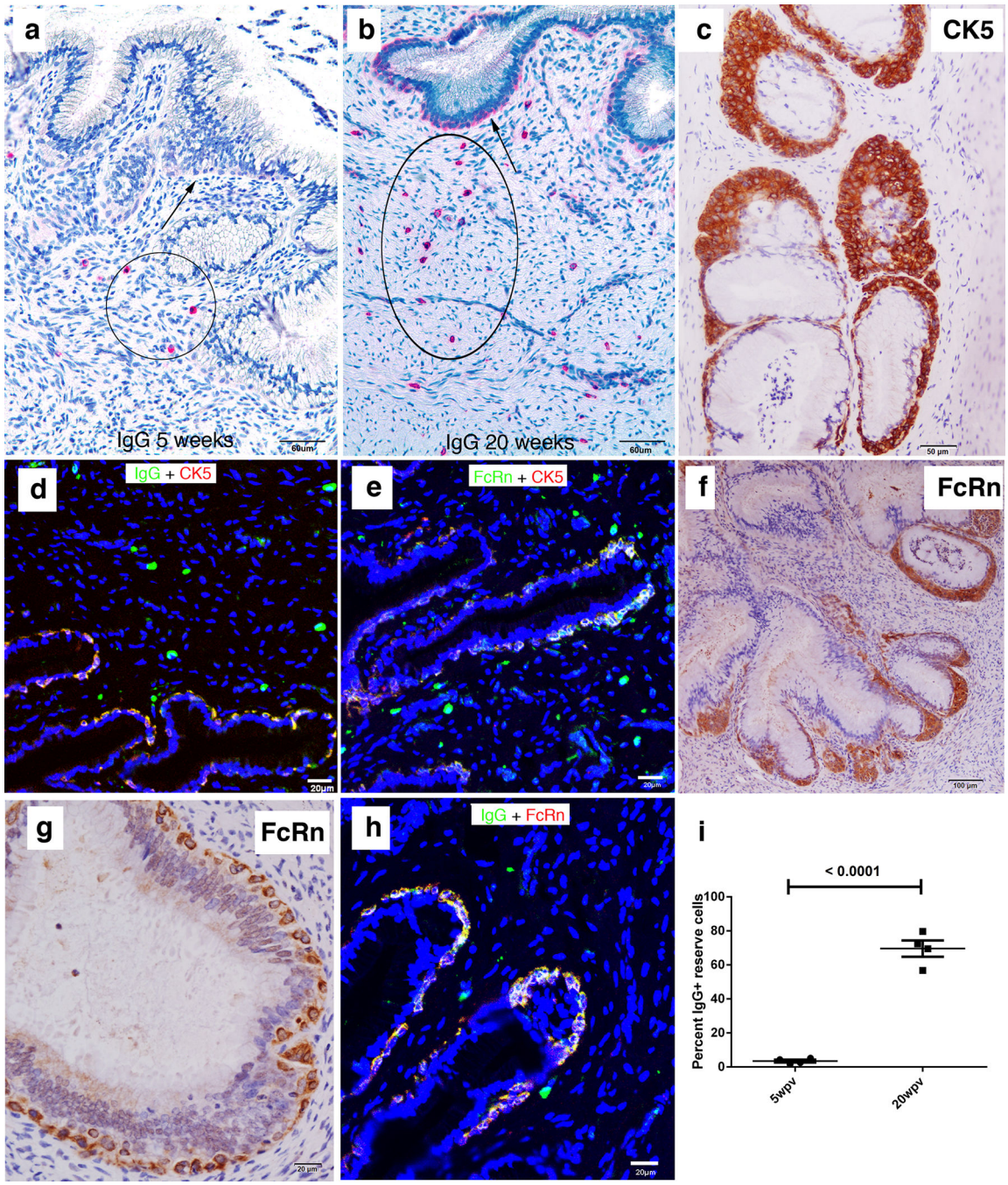

FIGURE 3.

Increases between 5 and 20 weeks in IgG^+ plasma cells, and IgG^+FcRn^+ cervical reserve epithelium. (**a, b**) Red-stained IgG^+ cells with plasma cell morphology (encircled) in the submucosa at 5 and 20 weeks. Arrows point to cells with epithelial morphology aligned beneath the columnar epithelium identified in (**c, d**) as cytokeratin 5 $(CK5)^+$ IgG^+ cervical reserve epithelium. (**e**) The $CK5^+$ cervical reserve epithelium is $FcRn^+$. (**f, g**) Brown-stained $FcRn^+$ cells with identical morphology and location beneath the columnar epithelium as $CK5^+$ cervical reserve epithelium shown in (**c**). (**h**) IgG is concentrated in the $FcRn^+$ reserve

epithelium. (**i**) Quantification of the relative numbers at 5 and 20 weeks of IgG^+ plasma cells in the submucosa and IgG^+ cervical reserve epithelium. Four animals analyzed at 5 weeks and four animals at 20 weeks.

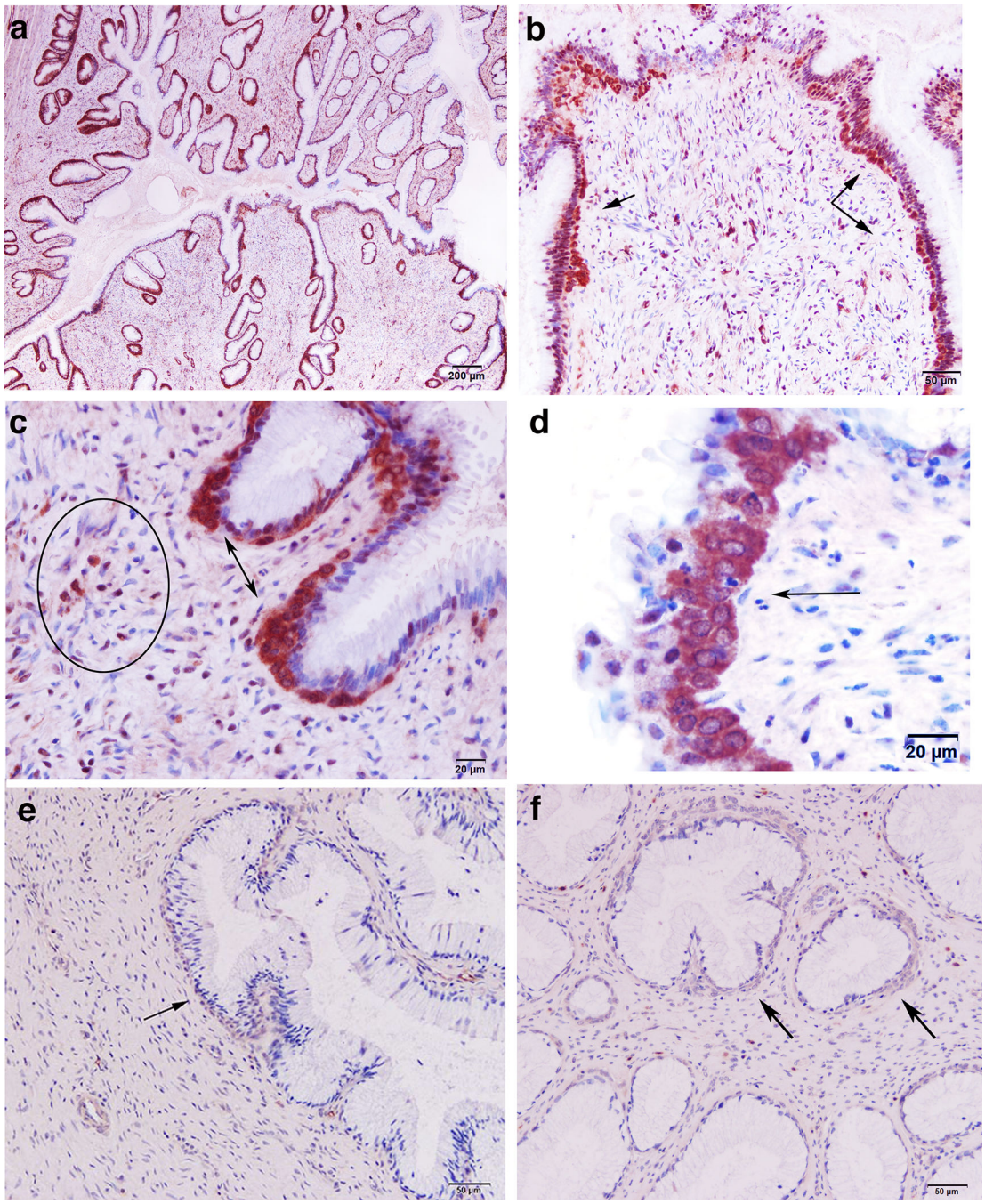

FIGURE 4.

Antibodies reactive with trimeric gp41 at 20 weeks in cervical reserve epithelium, plasma cells, and ectopic follicles. The soluble trimeric construct of gp41 (sgp41t) shown in Supplemental Figure 2 with a Strep-Tag for detection was used in RIHC to stain cells with antibodies reacting with sgp41t. (**a, b**) Brown-stained reserve epithelium beneath lining epithelium (arrows). (**c**) Brown-stained gp41t^{-} antibody^{+} reserve epithelium (double-headed arrows) and plasma cells (encircled). (**d**) High-power view of stained cervical reserve

epithelium (arrow) just below the columnar epithelium lining the cervix. (**e, f**) Background staining in two naïve controls. Arrows point to cervical reserve epithelium.

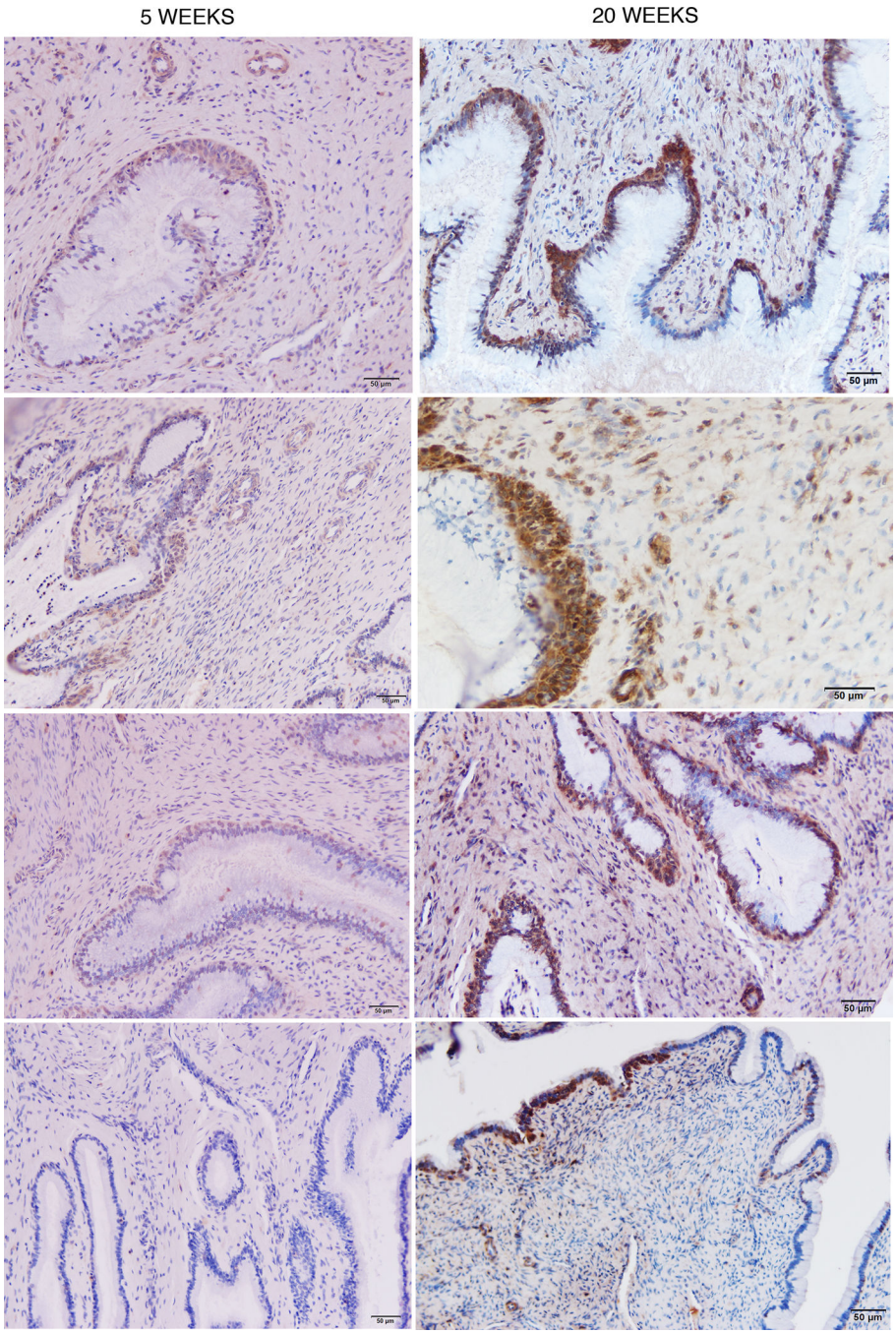

FIGURE 5.

Increased staining of gp41t antibody^{+} reserve cells at 20 weeks compared to 5 weeks. Each panel is from an individual animal.

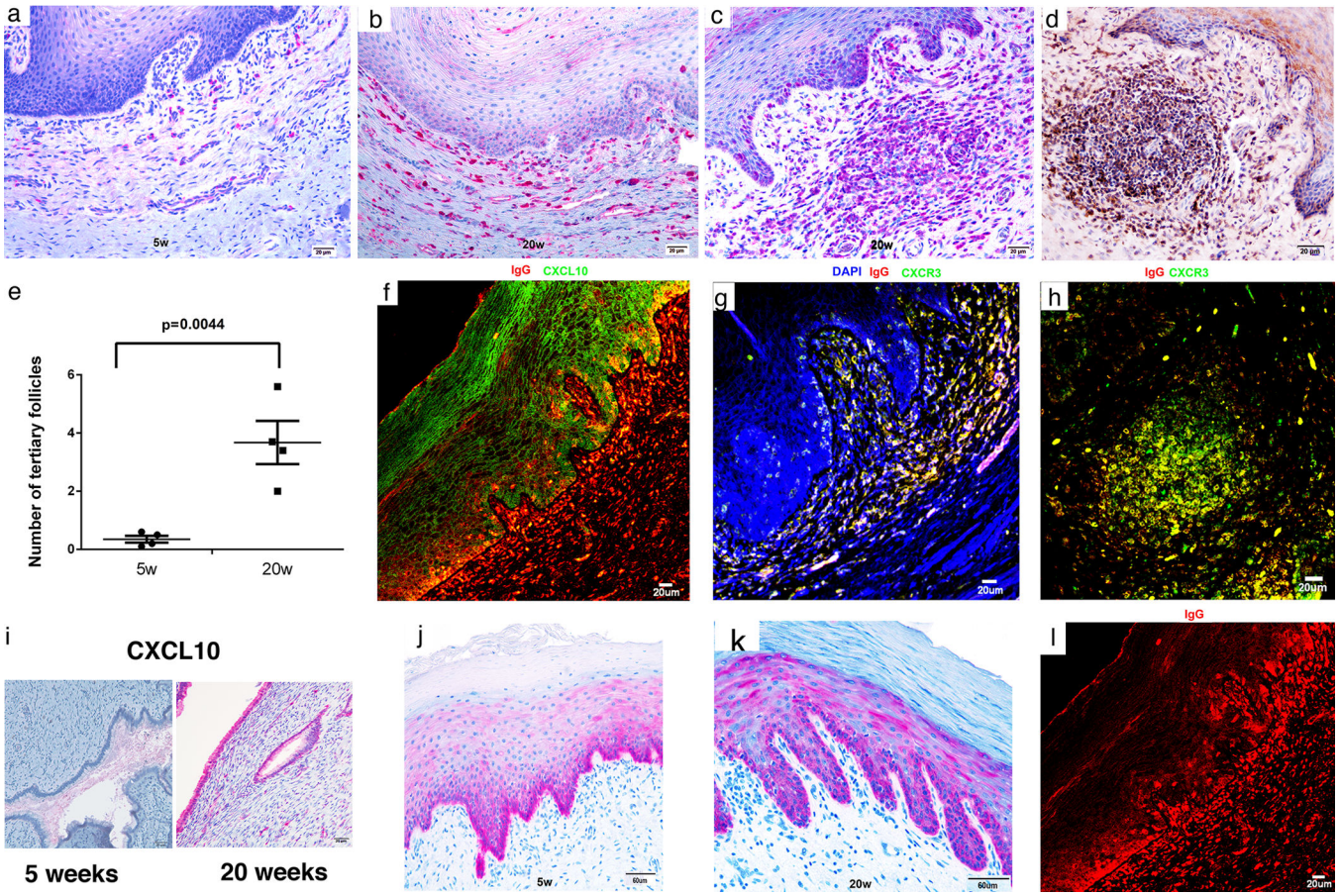

FIGURE 6.

Recruitment of plasma cells to vagina and cervix; induction of ectopic lymphoid follicles; and localization of IgG in FcRn$^+$ basal epithelium in the lower FRT. (**a,b**) Increased red-stained plasma cells in the submucosa at 20 weeks compared to 5 weeks. (**c–e**) Increases between 5 and 20 weeks in ectopic tertiary follicles in vagina. Follicles contain red-stained IgG$^+$ plasma cells in (**c**) and brown-stained gp41t-antibody$^+$ cells in (**d**). (**f–h**). Epithelial expression of CXCL10 and recruitment of CXCR3$^+$ plasma cells to the submucosa and ectopic follicles. In (**f**) CXCL10 expressing vaginal epithelium is stained green and the IgG in plasma cells is stained red. The orange appearance in the merged confocal micrograph is the result of IgG concentrated by the FcRn in CXCL10$^+$ basal epithelium (see also **j, k** and **l**). (**g, h**) CXCR3$^+$ IgG$^+$ plasma cells in the submucosa and in ectopic follicles are stained yellow. (**i**) Increased expression of CXCL10 between 5 and 20 weeks in red-stained endocervical epithelium. (**j,k**) Mainly basal epithelial expression of FcRn at 5 and 20 weeks. (**l**) IgG concentrated in the FcRn$^+$ epithelium above IgG$^+$ plasma cells. Image corresponds to (**f**) but only red-staining IgG shown.

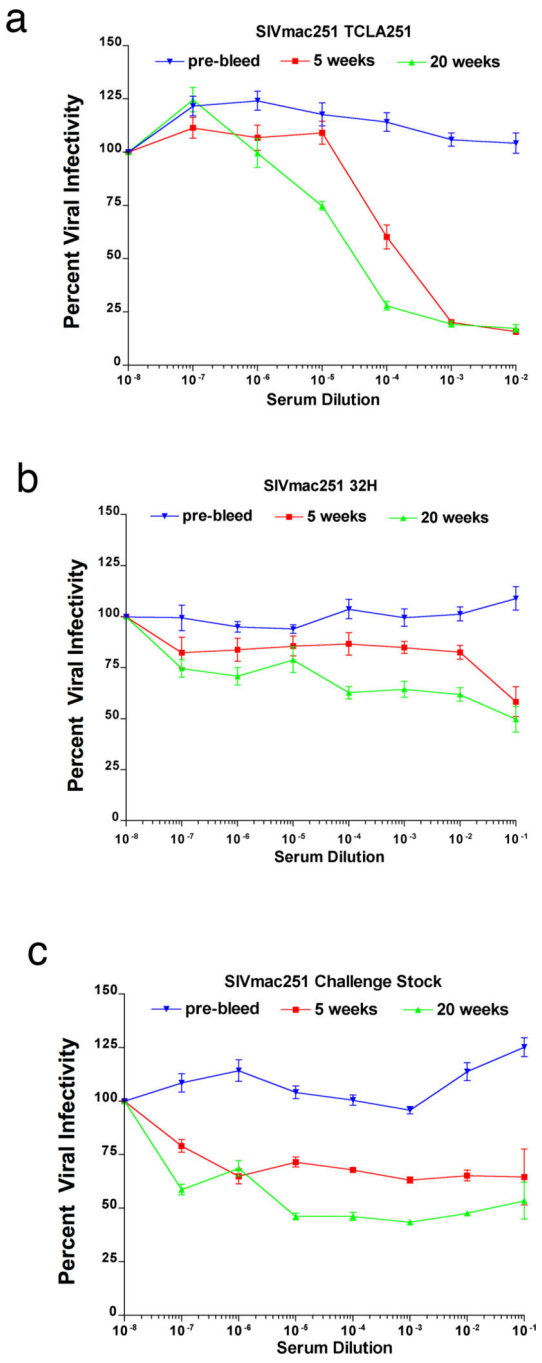

FIGURE 7.

Extracellular neutralization. (**a**) Sera neutralize tissue culture adapted (TCLA) SIVmac 251, at 20 weeks at higher titer compared to 5 weeks. (**b, c**) Compared to pre-bleed sera, $SIV_{mac251\text{-}32H}$ and the challenge stock of WT SIV_{mac251} are partially neutralized over a broad range of dilutions, to 50% reduction in infectivity with 20-week sera.

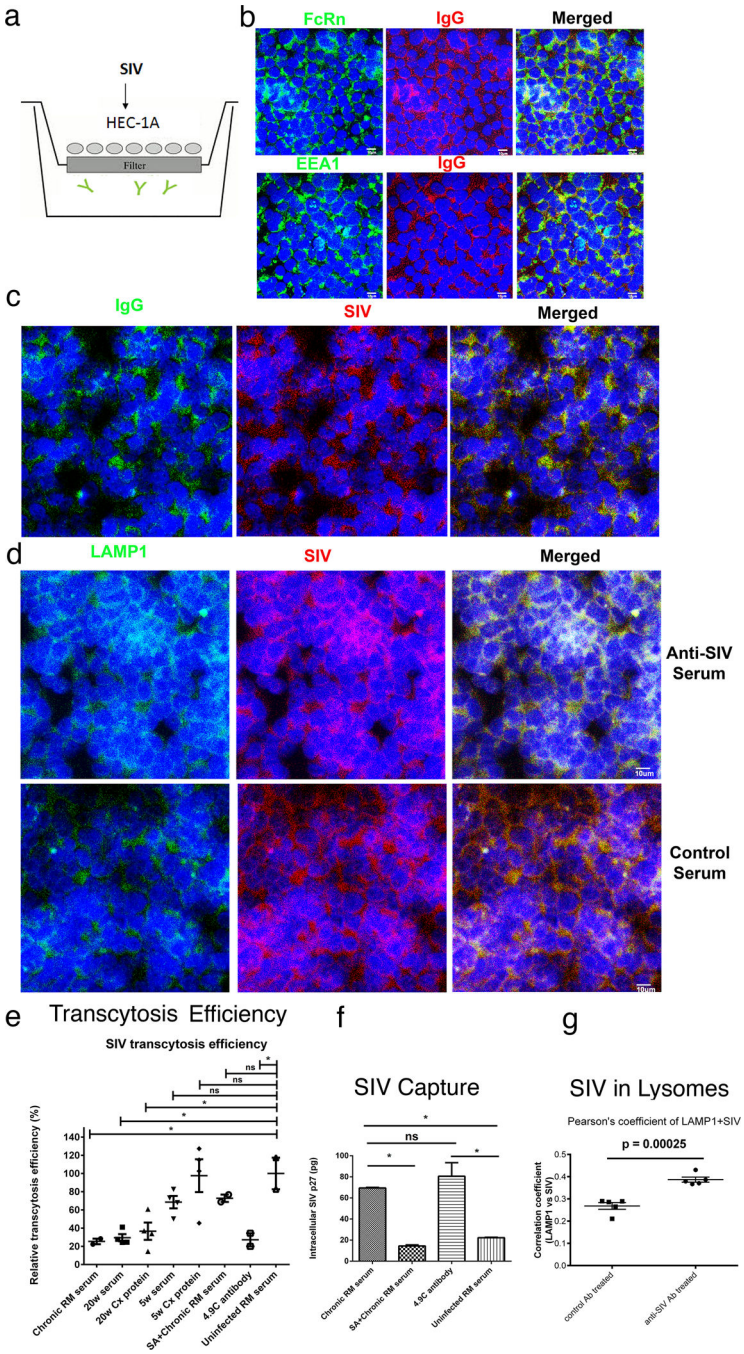

FIGURE 8.

Transcytosis, virus capture and intracellular neutralization (**a**). HEC 1-A-FcRn^{+} epithelial cell line and transwell system to assay SIV-capture, transcytosis and intracellular neutralization. SIV is added to the upper well. IgG antibodies (depicted as Y) are in the lower well (**b**) IgG and the FcRn co-localize in the EEA1^{+} early endosomal pathway. (**c, d**) SIV is captured in the FcRn transcytosis pathway and diverted to Lamp1^{+} lysosomes by anti-SIV sera but not control sera. (**e, f**) Quantification. Transcytosis of SIV in the transwell system is significantly decreased by antibodies from a SIV-infected rhesus macaque (RM);

and sera and a cervical tissue extract (Cx Protein) from an animal at 20 weeks post vaccination and the rhesus monoclonal antibody 4.9C, which reacts identically in WBs to the cervical tissue antibodies to oligomeric gp41. Sera and cervical tissue extract (Cx protein) at 5 weeks post vaccination, and sera from uninfected RM do not significantly decrease transcytosis. The FcRn-translocation pathway was required for capture and transcytosis, since Staphylococcal protein A (SA), which blocks the interaction between FcRn and IgG, (20–21), diminished viral capture and inhibitory effect on viral transcytosis by SIV-infected RM serum. (**g**). Co-localization of SIV with $LAMP1^{+}$ lysosomes in HEC 1-A cells treated with anti-SIV serum but not control serum from an uninfected animal. Extent of co-localization expressed as Pearson correlation coefficients. The small p values reflect the small group standard deviation relative to the magnitude of the difference between groups.

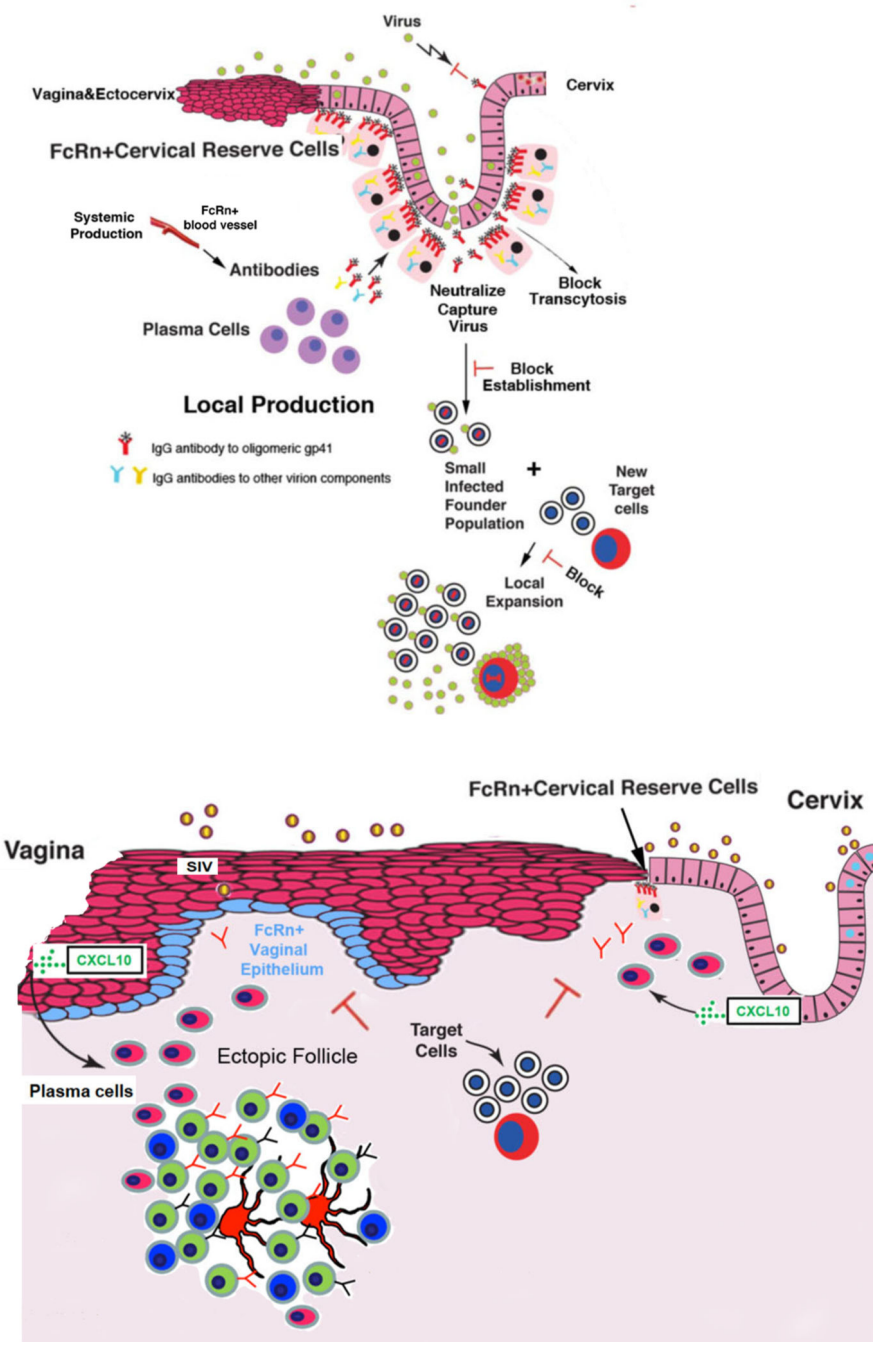

FIGURE 9.

Model of local production and FcRn-mediated delivery of antibodies and effects of anti-gp41t antibodies at the cervical (upper panel) and vaginal mucosal borders (lower panel). In the TZ and endocervix, IgG antibodies to trimeric gp41are produced by plasma cells. These antibodies are efficiently collected because of their spatial proximity to $FcRn^{+}$ cervical reserve epithelium, and thereby concentrated on the path of virus entry. The concentrated antibodies could then interfere by potentially several mechanisms with the establishment and expansion of infected founder populations. In both the vagina and cervix, mucosal epithelial

expression of CXCL10 recruits $CXCR3^+$ plasma cells. In the vagina, ectopic follicles are induced, and antibodies are produced by plasma cells in the submucosa and follicles. FcRn expression in the basal epithelium concentrates these IgG antibodies on the path of virus that has traversed the multilayer epithelium lining the vagina and ectocervix to prevent infection of target cells in the submucosa.